PNAS NEXUS

PNAS Nexus, 2025, 4, pgaf144
https://doi.org/10.1093/pnasnexus/pgaf144
Advance access publication 6 May 2025
Research Report

# Experimental infection of shrews (*Crocidura russula*) with Borna disease virus 1: Insights into viral spread and shedding

Daniel Nobach[a,b,*], Leif Raeder[a], Jana Müller[a], Sibylle Herzog[c], Markus Eickmann[d] and Christiane Herden[a,e,*]

[a]Institute of Veterinary Pathology, Justus-Liebig-University, Giessen 35392, Germany
[b]Chemical and Veterinary Analysis Agency Stuttgart (CVUAS), Schaflandstraße 3/2, Fellbach 70736, Germany
[c]Institute of Virology, Justus-Liebig-University, Giessen 35392, Germany
[d]Institute of Virology, Philipps-University, Marburg 35043, Germany
[e]Center for Mind, Brain and Behavior, Justus-Liebig-University, Frankfurterstraße 96, Giessen 35392, Germany
*To whom correspondence should be addressed. Email: daniel.nobach@cvuas.bwl.de (D.N.); Email: christiane.herden@vetmed.uni-giessen.de (C.H.)
**Edited By** Sam Telford, III

## Abstract

Numbers of human encephalitis cases caused by infection with Borna disease virus 1 (BoDV1) increase continuously in endemic areas. The reservoir host of BoDV1 is the bicolored white-toothed shrew, albeit few naturally infected individuals of other shrew species have been detected. To establish a reliable experimental reservoir model, 15 greater white-toothed shrews were infected with a shrew-derived BoDV1 isolate by different inoculation routes (intracerebral, intranasal, oral, subcutaneous, and intraperitoneal) and monitored up to 41 days. Except for the oral route, all other animals (12/15) were successfully infected, and the majority of them displayed temporarily reduced feed intake and loss of body weight but no inflammatory lesions. Infectious virus was isolated from 11/12 infected animals. Viral RNA was demonstrated by qRT-PCR in the central nervous system (CNS) and the majority of organs. Immunohistochemistry demonstrated BoDV1 antigen in neurons and astrocytes in the CNS and peripheral nerves. High viral loads in the CNS and the spinal cord points towards spread from periphery to the CNS to enhance viral replication and subsequent centrifugal spread to organs capable of secretion and excretions. In general, successful experimental BoDV1 infection of shrews proves their usefulness as animal model, enabling further studies on maintenance, transmission, pathogenesis, and risk assessment for human spillover infections.

**Keywords:** zoonotic infectious disease, reservoir, shrew, insectivore, host virus interactions

### Significance Statement

Numbers of human encephalitis cases caused by infection with Borna disease virus 1 (BoDV1) increase continuously. Local shrew populations are considered as natural source of infection. To understand the virus–reservoir interaction, a reliable animal model using shrews was established. Using different infection routes, the entry, viral spread, and shedding in shrews are enlightened. Despite lack of pathologic lesions and in contrast to chronic infections, in the acute phase of the BoDV1 infection shrews developed clinical signs. In further studies, this animal model will be useful for further understanding of mechanisms of tolerance of viruses in reservoirs and disease development.

## Introduction

Diseases caused by pathogens originating from wildlife reservoirs are considered an emerging worldwide public health hazard (1, 2). In Germany, increasing numbers of human encephalitis cases, caused by infection with Borna disease virus 1 (BoDV1), have been discovered in ongoing studies and by retrospective analyses of cases with previously unknown etiology (3–9).

BoDV1 is a negative-sensed single-stranded RNA virus (order *Mononegavirales*, family *Bornaviridae*, genus *Orthobornavirus*), which has long been known to infect a wide range of vertebrates (10). This includes primarily mammals and recently also humans, thereby substantiating its zoonotic capacity (3–5, 7, 9–12). Most identified natural cases occurred in domestic livestock, such as horses, sheep, and South American camelids (10, 13–16). Natural infections are epidemiologically associated with the presence of its natural reservoir, the bicolored white-toothed shrew (*Crocidura leucodon*) (6, 17–20). In accidental spillover hosts, BoDV1 infection can cause Borna disease, a severe neurological

**Competing Interest:** The authors declare no competing interests.
**Received:** October 28, 2024. **Accepted:** March 28, 2025

disorder with fatal meningoencephalitis and neurological symptoms, such as behavioral abnormalities, apathy, and ataxia (3–5, 9–11, 21). Similar to animal spillover hosts, human BoDV1 infections lead to a severe and mostly fatal encephalitis (3–5, 8, 22). The discovery of increasing numbers of acute human cases (>50 cases) demonstrates the impact of BoDV1 concerning public health (4, 7, 9, 22–24). However, the routes of transmission of BoDV1 to humans and associated factors have not yet been fully elucidated despite case–control studies (25).

Epidemiological characteristics, such as occurrence of natural infections in distinct endemic areas and higher incidence in certain years and months, have already pointed to a wildlife reservoir of BoDV1 (26–28). So far, the identified main reservoir is the bicolored white-toothed shrew (*C. leucodon*) (17–19, 29). The presence of BoDV1 in other European shrews such as the greater white-toothed shrew (*Crocidura russula*) and the lesser white-toothed shrew (*Crocidura suaveolens*) and that in one common shrew (*Sorex araneus*) have only recently been described, indicating either spillover events or potential additional wildlife reservoirs in some endemic areas (30, 31).

The widespread tissue distribution and shedding of BoDV1 combined with the lack of corresponding gross and histological changes in naturally infected *C. leucodon* support their role as BoDV1 reservoir. *Crocidura leucodon* harbors virus in nearly all organs, with the highest load in the central nervous system (CNS), and inflammation, especially encephalitis, and other CNS lesions or alterations in other organs are absent (18–20, 29). In contrast, BoDV1 is restricted to the CNS and peripheral nervous system in spillover hosts, where it causes a T-cell-based immune-mediated inflammation, markedly nonpurulent meningoencephalitis (3–5, 7, 11, 22). In persistently infected *C. leucodon*, virus presence and replication in organs such as kidney, skin, and salivary gland enable shedding via several routes such as saliva, urine, and skin secretions (20). Furthermore, clinical symptoms, as noted in spillover or dead-end hosts, are absent in *C. leucodon*. Persistently BoDV1-infected shrews show neither altered behavior nor changes in feed intake or weight, despite continuous viral shedding, widespread virus distribution, and presence of virus-specific serum antibodies (20). However, data on the transmission routes that ensure maintenance of BoDV1 in the reservoir population of *C. leucodon* are still lacking.

Infection research on BoDV1 infections has so far been hampered by the lack of suitable animal models for reservoir hosts. Various infection routes and the acute and chronic persistent phases of BoDV1 infections have already been studied extensively in spillover and experimental hosts, such as rats and mice (10, 13, 32, 33). In contrast, studies on details of BoDV1 infections of reservoir hosts are scarce. For other virus–reservoir interactions such as hantaviruses and their rodent reservoir hosts, transmission to humans through exposure to infected excreta is known, as well as the main route of transmission between rodents through aggressive interactions (34). Preventive strategies for spillover incidents could be developed based on these known risk factors (34). For BoDV1 infections, suitable shrew models for experimental studies detailing the route of infection, viral spread and distribution, and subsequent transmission within the reservoir population or to the spillover hosts are currently not available. Maintenance and breeding of *C. leucodon* as an insectivore species are more demanding than that of laboratory rodents and also in comparison with another shrew species of the genus Crocidura, the greater white-toothed shrew (*C. russula*). For *C. russula*, a successful captive breeding colony exists under laboratory conditions in our working group. Thus, this study aimed to establish and evaluate *C. russula* as a suitable and reliable shrew model for infection research on viruses, especially BoDV1.

*Crocidura russula* can be found close to and in human habitats in extensive agricultural areas in Europe, including endemic areas of BoDV1, such as Germany and Switzerland (35–37). The occurrence of *C. russula* and *C. leucodon* is considered partially sympatric with ecological separation, as the larger *C. russula* can displace the smaller *C. leucodon* (36, 38, 39). The recent detection of BoDV1 in wild *C. russula* raises the question whether this species can serve as a BoDV1 reservoir in general (30). In view of increasing numbers of human bornavirus infections and the unknown route of transmission, further investigations into the reservoir and host–virus interactions are therefore urgently required. For this reason, the objectives of this study were as follows: firstly to assess the feasibility of *C. russula* as shrew model for BoDV1 infections and secondly to characterize acute BoDV1 infections of *C. russula* with focus on different infection routes, clinical outcome, immune response, and viral shedding.

## Materials and methods

### Ethics

The animal experiment was evaluated and approved by the ethics committee of the Regierungspräsidium Gießen (AZ G38/2018). All procedures were conducted in approved biosafety level 2 facilities according to animal welfare guidelines of the American Society of Mammalogist (40) adopted to shrew husbandry.

### Animal study

Greater white-toothed shrews (*C. russula*) were bred at the Animal Facility of the Philipps-University Marburg licensed by the administrative district of Marburg-Biedenkopf (Az LRV FD 83.4.1-19c 20/21). Adult male and female shrews were infected via five different inoculation routes (oral, intranasal, subcutaneous, intraperitoneal, and intracerebral) with a group size of three animals each. Infection was performed under general anesthesia with isoflurane (induction 4% flow, maintenance 2% flow). All animals received at least 10 µL BoDV1 virus suspension (corresponding to virus dose of 6,000 $ID_{50}$). The virus was originally isolated from skin swabs of a naturally infected white-toothed shrew in rabbit embryonic brain cells (20) and was passaged two times before infection. For oral inoculation, virus suspension was dropped onto the buccal mucosa; for nasal inoculation, virus suspension was dropped onto the nasal orifices; for the other inoculation routes, a suitable syringe was used and the medium volume was increased to 100 µL for subcutaneous and intraperitoneal application. The animals were weighed weekly and scored daily for clinical signs according to the adopted score sheet (Table S1), and feed intake was measured over a period of 41 days. Shrews were euthanized if moderate impairment of the animal's welfare (as determined by scoring) was observed, or at the end of the study (day 41 postinfectionem [p.i.]) Additionally, oral swabs, skin swabs, and feces were collected weekly under anesthesia to monitor for virus shedding.

### Processing of tissues

At necropsy, the following tissues were collected for histopathology and immunohistochemistry and for RNA isolation and BoDV1-RT-PCR: cerebral cortex, hippocampus, olfactory bulb, brain stem, hippocampus, spinal cord (not for RNA isolation), brachial plexus, sciatic nerve, nasal conchae, parotid salivary gland, sublingual salivary gland, lung, heart, liver, spleen, kidney, urinary bladder, esophagus, stomach, small intestine (duodenum),

**Table 1.** Overview over collected tissues at necropsy.

| BoDV1 RNA (qRT-PCR) | Serum antibodies (IIFT) | Infectious virus (virus isolation) | BoDV1 antigen [IHC] |
|---|---|---|---|
| Brain (cerebral cortex) | Blood | Blood | Brain (cerebral cortex) |
| Brain (hippocampus) | | Brain (hippocampus) | Brain (hippocampus) |
| Brain (olfactory bulb) | | Lung | Brain (olfactory bulb) |
| Brain (brain stem) | | Liver | Brain (brain stem) |
| Brain (cerebellum) | | Kidney | Brain (cerebellum) |
| Peripheral nerve/plexus brachialis | | Urinary bladder | Peripheral nerve/ plexus brachialis |
| Peripheral nerve/ischiatic nerve | | Parotid salivary gland | Peripheral nerve/ ischiatic nerve |
| Spinal cord (thoracal) | | Flank dermal gland | Spinal cord (cervical) |
| Parotid salivary gland | | | Spinal cord (thoracal) |
| Sublingual salivary gland | | | Spinal cord (lumbar) |
| Nasal conchae | | | Parotid salivary gland |
| Lung | | | Sublingual salivary gland |
| Esophagus | | | Nasal conchae |
| Stomach | | | Lung |
| Small intestine | | | Stomach |
| Large intestine | | | Small intestine |
| Liver | | | Large intestine |
| Spleen | | | Liver |
| Bone marrow | | | Pancreas |
| Kidney | | | Spleen |
| Urinary bladder | | | Kidney |
| Genital tract | | | Genital tract |
| Adrenal gland | | | Adrenal gland |
| Skin | | | Skin |
| Flank dermal gland | | | Flank dermal gland |
| Skeletal muscle | | | Brown fat tissue |
| Heart | | | Heart |

IIFT, indirect immunofluorescence test; IHC, immunohistochemistry.

large intestine (colon), adrenal gland, genital tract (testis or ovary), skeletal muscle (hind leg), bone marrow (femur), dermal flank gland, and skin (abdomen) (overview in Table 1). For RNA isolation, tissues were taken aseptically and processed with Qiazol and RNeasy Mini Kit according to manufacturer's guide. Blood was collected postmortem and processed for detection of BoDV1-reactive serum antibodies. Additionally, a subset of tissues (hippocampus, lung, liver, kidney, urinary bladder, parotid gland, and dermal flank gland) and blood were collected for infectivity tests as described previously (41). Furthermore, sections of the above-mentioned tissues were fixed in 4% neutral-buffered formalin, embedded in paraffin, and processed for histopathology and immunohistochemistry.

RNA from oral swabs, skin swabs, and feces was extracted with RNeasy Mini Kit according to manufacturer's guide in an elution volume of 600 µL lysis buffer.

## Detection of BoDV1 RNA by qRT-PCR

BoDV1 RNA was detected by qRT-PCR using BoDV1 primers and probe according to Schlottau et al. (3). qRT-PCR runs were performed on Rotorgene Q (Qiagen) with SensiFAST Probe No-ROX One-Step Kit (Meridian Bioscience, formerly Bioline) according to manufacturer's guide. The BoDV1 specific mix was combined with an internal beta-actin control mix to assess sample quality. A quantified BoDV1 standard curve and nontemplate controls were included in each qRT-PCR run.

## Detection of bornavirus-reactive serum antibodies

Presence of bornavirus-reactive serum antibodies was investigated by indirect immunofluorescence assay as described elsewhere (18).

## Infectivity test

Infectious BoDV1 was assessed by virus isolation with rabbit embryo brain cells followed by direct immunofluorescence test as described elsewhere (41, 42). Upon detection of contamination (e.g. mycotic overgrowth), tissues were subsequently excluded from virus isolation and infectivity testing.

## Histology and detection of BoDV1 antigen by immunohistochemistry

The above-mentioned tissues were examined histologically for the presence of inflammatory and/or degenerative lesions by two veterinary pathologists (D.N. and L.R.). Immunohistochemistry was performed applying the monoclonal antibody Bo18 detecting the BoDV1 nucleoprotein as described elsewhere (18). Antigen distribution and the number of infected cells were graded independently by two veterinary pathologists (D.N. and L.R.) according to the score established elsewhere (43). An additional thorough interpretation of the antigen distribution within the spinal cord was performed by a board-certified pathologist (J.M.).

The experimental BoDV1 infection was considered successful if viral RNA and/or antigen was detected. Viral shedding was assessed positive in the case of presence of infectious virus in swabs and/or tissues and/or by demonstration of viral RNA.

# Results

Experimental BoDV1 infection was successful via intranasal (3/3), subcutaneous (3/3), intraperitoneal (3/3), and intracerebral (3/3) inoculation of BoDV1 in greater white-toothed shrews and not successful in orally inoculated animals (0/3). This indicates that experimental BoDV1 infection is easily possible in *C. russula* via different routes.

Most of the infected shrews displayed temporarily reduced feed intake and/or loss of body mass over the time course of the entire experiment (days 21 to 41, Fig. 1). A first phase of reduced feed intake was observed in the 7 days immediately following BoDV1 infection performed under anesthesia. However, no significant loss of body mass or other clinical signs, particularly neurological signs, were observed in any of the animals in these first days. From day 21 p.i. (dpi) onward, a total of seven animals had to be euthanized due to reduced feed intake and body mass. Specifically, this involved one intranasally infected shrew on 28 dpi due to reduced feed intake and a loss of up to 23% of its starting body mass. In addition, two other shrews (one subcutaneously and one intraperitoneally infected animal) were removed from the experiment after 28 dpi for the same reasons, as were one intranasally infected and all intracerebrally infected animals from 35 dpi onward (Table 2). None of the shrews showed any other obvious disturbance of general condition or clinical signs, other than the reduction of feed intake (40 to 60% of normal intake) and body mass.

Infected shrews developed antibody titers of bornavirus-reactive serum antibodies ranging between 1:20,480 and 1:40,960 (Table 2) at the respective end point of the experiment without any significant difference between the animal groups.

In general, at the respective end point of the infection, viral RNA was consistently demonstrated by qRT-PCR in most organs, except for liver and spleen (Fig. 2) in all infected cohorts (details in Table S2). Overall, the viral load was highest in the CNS of intracerebrally (i.c.) infected shrews with $2 \times 10^{10}$ to $6 \times 10^{8}$ copies on 35 dpi. In the other groups, the highest viral load was also found in the CNS, ranging from $1 \times 10^{10}$ to $1 \times 10^{7}$ copies in the intranasal group, from $8 \times 10^{8}$ to $1 \times 10^{6}$ copies in the subcutaneous group, and from $5 \times 10^{8}$ to $1 \times 10^{6}$ copies in the intraperitoneal group.

In the intranasally infected group, viral load was high in the nasal conchae ($4.1 \times 10^{5}$–$1.3 \times 10^{9}$ copies) but only one animal had detectable viral load in the lung (H53, $8.21 \times 10^{6}$ copies). In all infected animals, viral copy numbers were generally higher in the nasal conchae ($1 \times 10^{9}$–$5 \times 10^{4}$) in contrast to the lung ($2 \times 10^{7}$–$3 \times 10^{4}$ copies).

Two animals of the intranasally infected group show no detectable viral load in most of organs of the abdomen (small intestine, large intestine, liver, spleen, kidney, urinary bladder, and adrenal glands), in contrast to the other groups.

In the spleen, virus RNA was detected in a total of five animals (H16, H41, H48, H52, and H53) with the highest copy number in an intraperitoneally infected animal (H48, $7.04 \times 10^{6}$ copies). In the liver, no viral RNA was found in any infected shrew.

Concerning oral swabs, skin swabs, and feces, BoDV1 RNA was first detected in a skin swab of a subcutaneously infected shrew at 35 dpi, followed by a positive skin swab of an intranasally infected shrew at 41 dpi, and detection in feces of a subcutaneously infected shrew at 41 dpi. Additionally, infectious virus was detected in oral swabs of two intracerebrally infected shrews at 35 dpi (Fig. 3).

In general, infectious virus was consistently isolated from all successfully infected animals except one intraperitoneally infected animal. Isolation was successful from the CNS and additionally from other organs such as lung, parotid salivary gland, urinary bladder, kidney, liver, and blood (Fig. 2).

Euthanasia-associated lesions, such as alveolar edema and hemorrhage, were observed in all animals on gross and histopathological examination. In contrast, none of the BoDV1-infected animals showed typical BoDV1 infection–associated lesions described in the CNS of accidental hosts, such as inflammation or degeneration. Moreover, no gross or histological alterations were found in any other organ system examined.

BoDV1 antigen, demonstrated by immunohistochemistry, was predominantly found in both the cytoplasm and nucleus of neurons and astrocytes in the central and peripheral nervous system, including myenteric ganglia and chromaffin cells of the adrenal medulla (Table 3 and Fig. 4). The immunohistochemistry score of BoDV1 antigen generally correlated with the viral copy number. The highest numbers of positive cells in the brain were found in intracerebrally and intranasally infected shrews. Both gray and white matter was affected, and in the hippocampus, antigen was found intracytoplasmic and intranuclear in neurons and astrocytes, as well as in the neuropil. In the cerebral cortex, antigen was present intracytoplasmically and intranuclearly in neurons and astrocytes. In the brain stem, clusters of neurons and astrocytes displayed intracytoplasmic and intranuclear antigen. Few cerebellar Purkinje cells, including their axons, harbored intracytoplasmic and intranuclear antigen, and the molecular layer was spared. Notably, one subcutaneously infected animal (H52) displayed no positive cells in the cerebellum, while antigen was found in neurons and astrocytes in the cerebral cortex, hippocampus, and brain stem. In the olfactory bulb, antigen was found intracytoplasmically and intranuclearly in neurons and astrocytes in all successfully BoDV1-infected groups, but not necessarily in every individual animal of the group. Thus, all intranasally and all intracerebrally infected animals displayed antigen-positive cells in this region, whereas BoDV1 antigen was not consistently detected in each of the subcutaneously and intraperitoneally infected animals.

In the spinal cord, all intranasally infected animals, as well as each two of the intraperitoneally, intracerebrally, and subcutaneously infected animals, displayed decreasing BoDV1-N distribution and number of positive cells from the cervical to the lumbar spinal cord. One subcutaneously and one intracranially infected animal displayed comparable distribution and number of positive cells throughout the whole spinal cord. Both gray and white matter was affected in all those animals, including motor neurons, glia cells, and surrounding neuropil with cellular processes. Additionally, dorsal root ganglia and, if evaluable, nerve fibers within the surrounding skeletal muscle were consistently positive. Notably, a mediodorsal triangular area within the dorsal funiculus of the spinal cord was relatively spared in evaluation of BoDV1-N-antigen distribution, displaying consistently less or no positive fibers (Fig. 5). In one intraperitoneally infected animal, BoDV1-N-antigen was not detected in any section and part of the spinal cord, except for a centrally located neuron and its immediate surrounding neuropil within the thoracic gray matter, and unilaterally, very few nerve fibers ventrally of and surrounding the thoracic vertebral column.

In all infected cohorts, peripheral nerve fibers in parotid and sublingual salivary gland, lung, kidney, skin, uterus, testis, and heart displayed BoDV1-N-antigen, as well as myenteric ganglia in the stomach and intestine.

Besides nervous tissue, epithelial and mesenchymal cells occasionally displayed BoDV1 antigen both intracytoplasmically and intranuclearly in all infected cohorts. Occasionally, epithelial cells of the parotid and sublingual salivary gland displayed viral antigen, as well as epithelial cells of the lingual taste papillae. Besides nerve fibers of the skin and lung, antigen was also found in epidermal keratinocytes and bronchial epithelial cells, respectively. Additionally, some pancreatic islets cells and mesenchymal cells of the brown fat tissue harbored BoDV1-N antigen. There was no perceptible difference between the infection groups in these above-mentioned tissues. In the nasal conchae, viral antigen was observed in nerve fibers and olfactory epithelial cells of the

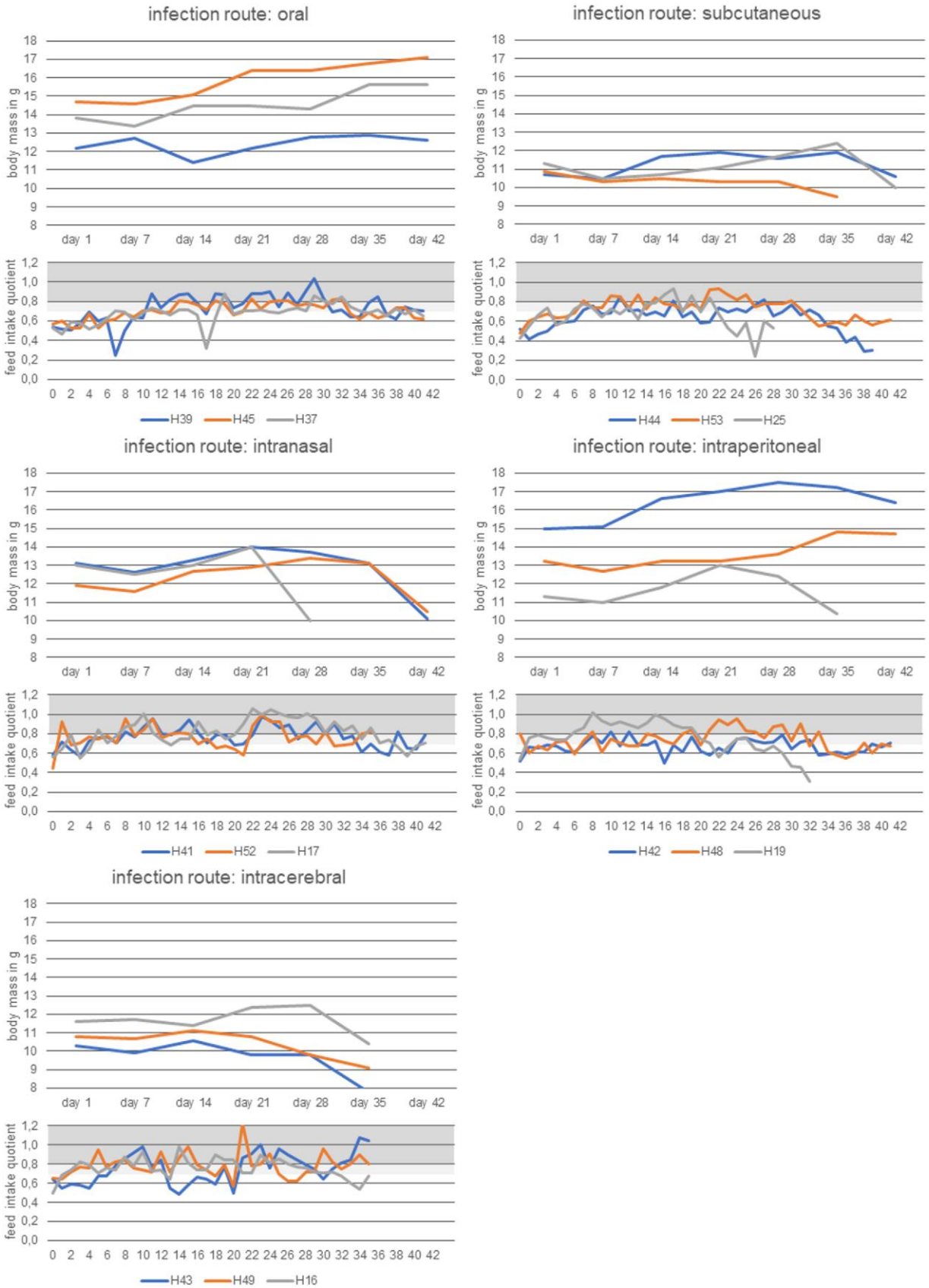


**Fig. 1.** Development of body mass and feed intake during infection in shrews experimentally infected with BoDV1. Feed intake quotient is the quotient of daily feed intake and body mass. Dark gray area (feed intake quotient >0.8) is considered normal intake; light gray area (feed intake quotient between 0.7 and 0.8) is considered lightly reduced intake.

**Table 2.** Animals and characteristics of infection.

| ID | Sex | Route of infection | End of trial[a] (dpi) | Titer of serum antibodies against BoDV1 | Detection of BoDV1 in brain[b] |
|---|---|---|---|---|---|
| H39 | Female | Oral | 41 | <1:10 | No |
| H45 | Male | Oral | 41 | <1:10 | No |
| H37 | Female | Oral | 41 | <1:10 | No |
| H44 | Female | Intranasal | 39 | 1:20,480 | Yes |
| H53 | Male | Intranasal | 41 | 1:40,960 | Yes |
| H25 | Male | Intranasal | 28 | 1:40,960 | Yes |
| H41 | Female | Subcutaneous | 41 | 1:40,960 | Yes |
| H52 | Female | Subcutaneous | 35 | 1:40,960 | Yes |
| H17 | Male | Subcutaneous | 41 | 1:40,960 | Yes |
| H42 | Male | Intraperitoneal | 41 | <1:10 | No |
| H48 | Male | Intraperitoneal | 41 | 1:20,480 | Yes |
| H19 | Female | Intraperitoneal | 33 | 1:40,960 | Yes |
| H43 | Female | Intracerebral | 35 | 1:40,960 | Yes |
| H49 | Female | Intracerebral | 35 | 1:40,960 | Yes |
| H16 | Male | Intracerebral | 35 | 1:20,480 | Yes |

ID, identification number.
[a]End of trial before 41 dpi was due to welfare score.
[b]Detection of BoDV1 RNA via qRT-PCR and/or BoDV1-N-antigen via immunohistochemistry.

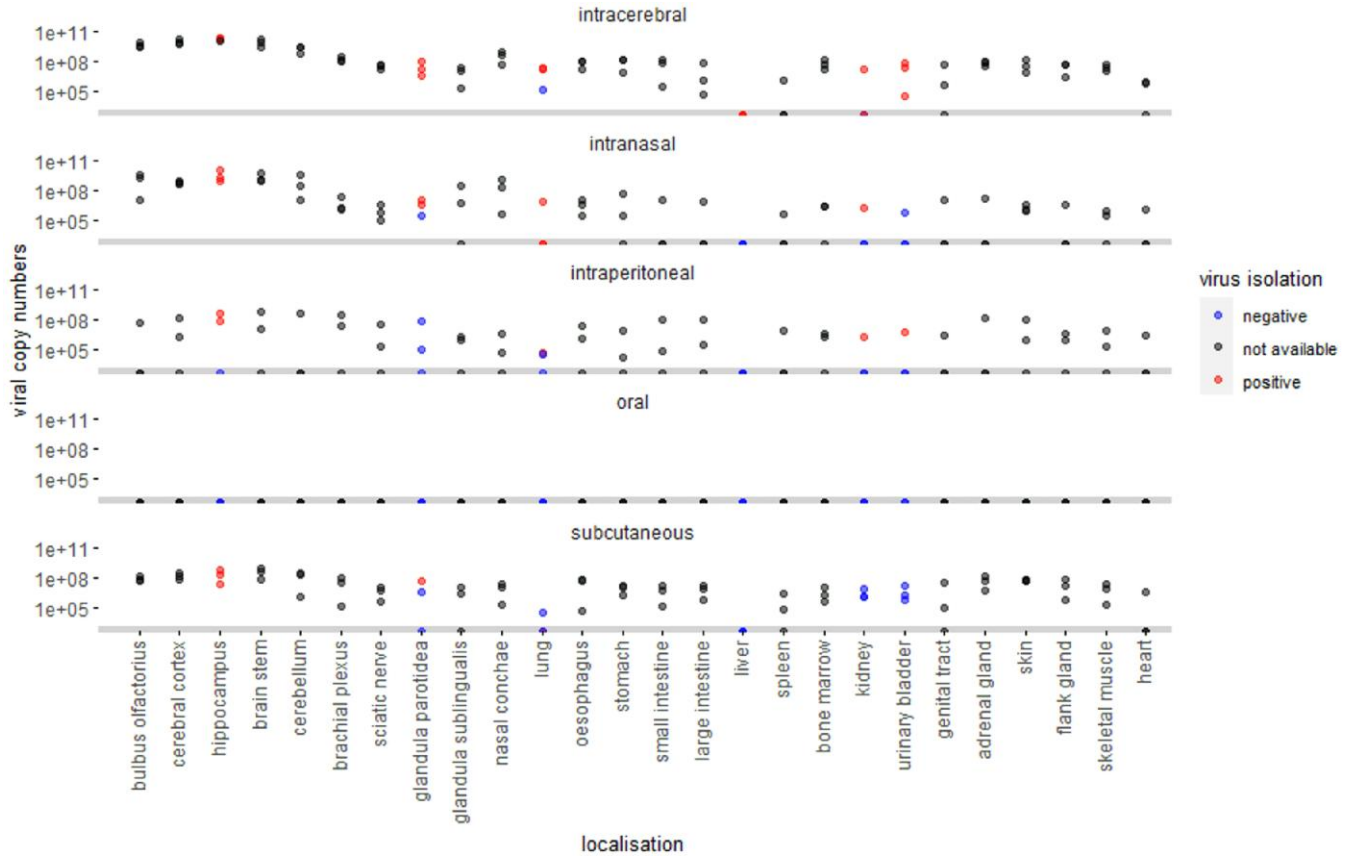


**Fig. 2.** Overview of viral load in tissues and virus isolation in shrews experimentally infected with BoDV1 via different infection routes (intracerebral, intranasal, intraperitoneal, oral, and subcutaneous). The gray area depicts viral copy numbers below the lower limit (<1,000 viral copies) and corresponds to $C_q$ values below cycle 35. Blue and red dots represent unsuccessful and successful BoDV1 isolation, respectively. Gray dots represent tissue from which virus isolation was not performed or not available due to contamination (termed not available).

intracerebrally and intranasally infected animals, whereas subcutaneously infected animals displayed antigen solely in nerve fibers.

## Discussion

Emerging and reemerging diseases caused by pathogens originating from wildlife reservoirs are of major concern for public health worldwide (1, 2). Next to human health, One-Health approaches also put a spotlight on the environment, as well as on domestic animals and wildlife in their natural habitats (24, 25). Due to the availability of various high-throughput methods, such as metagenomics, our knowledge of potential pathogens, as well as spillover and reservoir host species, is constantly expanding (1, 44) and may potentially extend to include additional currently unknown animal, human, and environmental factors.

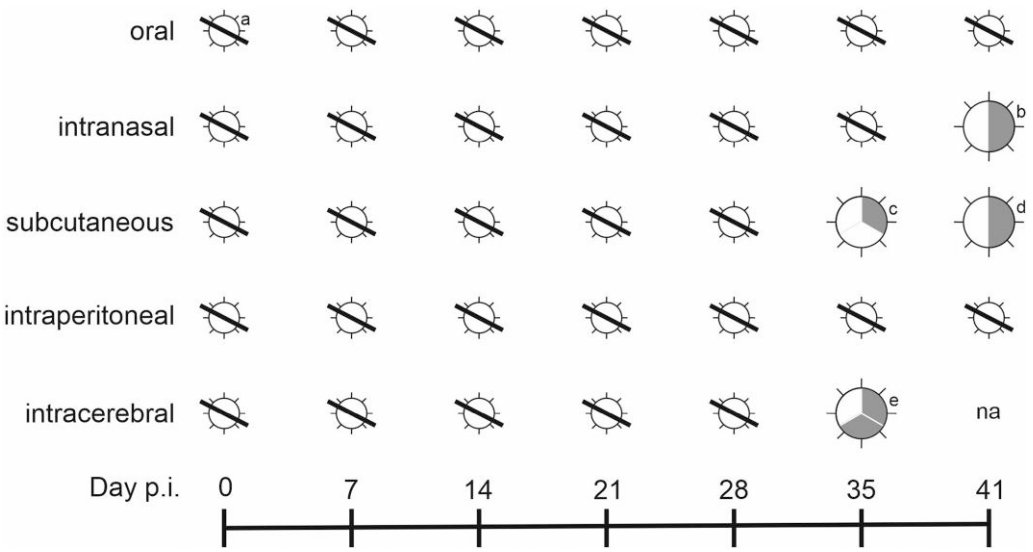


**Fig. 3.** Schematic representation of detection of BoDV1 RNA and infectious virus in skin swabs, oral swabs, and feces. a) no detection, b) day 41, one of two intranasally infected shrews with RNA in skin swabs, no RNA, or infectious virus in other swabs, c) day 35, one of three subcutaneously infected shrews with RNA in skin swab, no RNA, or infectious virus in other swabs, d) day 41, one of two subcutaneously infected shrews with RNA in feces, no RNA, or infectious virus in other swabs, and e) day 35, two of three intracerebrally infected shrews with infectious virus in oral swabs, no RNA, or infectious virus in other swabs. na, not available.

**Table 3.** Demonstration of BoDV1 antigen distribution by immunohistochemistry.

| Infection route | Oral | | | Intranasal | | | Subcutaneous | | | Intraperitoneal | | | Intracerebral | | |
|---|---|---|---|---|---|---|---|---|---|---|---|---|---|---|---|
| Animal | H39 | H45 | H37 | H44 | H53 | H25 | H41 | H52 | H17 | H42 | H48 | H19 | H43 | H49 | H16 |
| Olfactory bulb | 0 | 0 | 0 | 2 | 3 | 2 | 2 | 0 | 2 | 0 | 2 | 0 | 2 | 2 | 4 |
| Cerebral cortex | 0 | 0 | 0 | 2 | 4 | 3 | 3 | 2 | 2 | 0 | 2 | 1 | 4 | 4 | 4 |
| Hippocampus | 0 | 0 | 0 | 3 | 4 | 3 | 3 | 2 | 3 | 0 | 1 | 2 | 4 | 4 | 4 |
| Brain stem | 0 | 0 | 0 | 2 | 3 | 2 | 2 | 2 | 3 | 0 | 2 | 2 | 3 | 3 | 4 |
| Cerebellum | 0 | 0 | 0 | 3 | 2 | 1 | 1 | 0 | 1 | 0 | 1 | 1 | 1 | 2 | 3 |
| Spinal cord (cervical) | 0 | 0 | 0 | 3 | 3 | 2 | 4 | 2 | 4 | 0 | 4 | 3 | 4 | 4 | 4 |
| Spinal cord (thoracal) | 0 | 0 | 0 | 1 | 2 | 1 | 4 | 1 | 4 | 1 | 3 | 2 | 3 | 4 | 3 |
| Spinal cord (lumbar) | 0 | 0 | 0 | 1 | 2 | 1 | 3 | 0 | 4 | 0 | 2 | 1 | 2 | 3 | 2 |
| Peripheral nerve/plexus brachialis | 0 | 0 | 0 | 1 | 3 | 2 | 2 | 2 | 3 | 0 | 2 | 1 | 3 | 3 | 2 |
| Peripheral nerve/ischiatic nerve | 0 | 0 | 0 | 0 | 2 | 0 | 1 | 0 | 1 | 0 | 2 | 0 | 2 | 2 | 1 |
| Parotid salivary gland | 0 | 0 | 0 | 0 | 1 | 0 | 1 | 0 | 1 | 0 | 1 | na | 0 | 2 | 1 |
| Sublingual salivary gland | 0 | 0 | 0 | na | 1 | 0 | 1 | 0 | 1 | 0 | 1 | na | 0 | 1 | 1 |
| Nasal conchae | 0 | 0 | 0 | 1 | 3 | 0 | 0 | 0 | 1 | 0 | 0 | 0 | 0 | 3 | 2 |
| Lung | 0 | 0 | 0 | 0 | 1 | 0 | 1 | 0 | 1 | 0 | 1 | 0 | 0 | 1 | 1 |
| Stomach | 0 | 0 | 0 | 1 | 1 | 0 | 1 | 1 | 1 | 0 | 1 | 1 | 1 | 1 | 1 |
| Small intestine | 0 | 0 | 0 | 0 | 1 | 0 | 1 | 1 | 1 | 0 | 1 | 0 | 0 | 1 | 1 |
| Large intestine | 0 | 0 | 0 | 0 | 1 | 0 | 1 | 0 | 1 | 0 | 1 | 0 | 0 | 1 | 1 |
| Liver | 0 | 0 | 0 | 0 | 1 | 0 | 0 | 0 | 0 | 0 | 1 | 0 | 0 | 0 | 0 |
| Pancreas | 0 | 0 | 0 | 0 | 0 | 0 | 0 | 0 | 0 | 0 | 1 | na | 0 | 1 | 0 |
| Spleen | 0 | 0 | 0 | 0 | 0 | 0 | 0 | 0 | 0 | 0 | 0 | 0 | 0 | 0 | 0 |
| Kidney | 0 | 0 | 0 | 0 | 1 | 0 | 1 | 0 | 1 | 0 | 0 | 0 | 0 | 0 | 0 |
| Testis/uterus | 0 | 0 | na | 0 | 1 | 0 | 1 | 0 | 0 | 0 | 1 | 0 | 0 | 2 | 0 |
| Adrenal gland | na | 0 | 0 | 0 | 1 | 0 | 1 | 0 | 1 | 0 | 1 | 0 | 0 | na | 1 |
| Skin | 0 | 0 | 0 | 0 | 2 | 0 | 1 | 0 | 2 | 0 | 2 | 0 | 1 | 2 | 1 |
| Flank gland | 0 | 0 | na | 0 | 0 | 0 | 1 | na | 0 | 0 | 1 | 0 | na | 2 | 1 |
| Brown fat tissue | 0 | 0 | 0 | 0 | 1 | 0 | 1 | 0 | 0 | 0 | 1 | 0 | 0 | 1 | 0 |
| Heart | 0 | 0 | 0 | 0 | 0 | 0 | 0 | 0 | 0 | 0 | 1 | 0 | 0 | 1 | 1 |

0, no positive cells; 1, low number of positive cells (1–15% of the sectioned tissue, 1–30 cells); 2, moderate number of positive cells (15–40%, 30–80 cells); 3, high number of positive cells (40–65%, 80–150 cells); 4, very high number of positive cells (>65%, >150 cells), score according to Petzold et al. (43); na, not available.

In Germany, increasing numbers of human encephalitis cases caused by infection with BoDV1 have raised the awareness und urgent need to understand underlying pathogen–reservoir host interactions and potential spillover events (4, 6, 23). Besides sampling of naturally infected shrew species, detailed studies were hampered due to the lack of suitable animal and in vitro models to investigate the reservoir situation. On the contrary, models for the analysis of the dead-end host status, with viral restriction to the CNS and concomitant nonpurulent meningoencephalitis based on T-cell-mediated immunopathology, have been widely

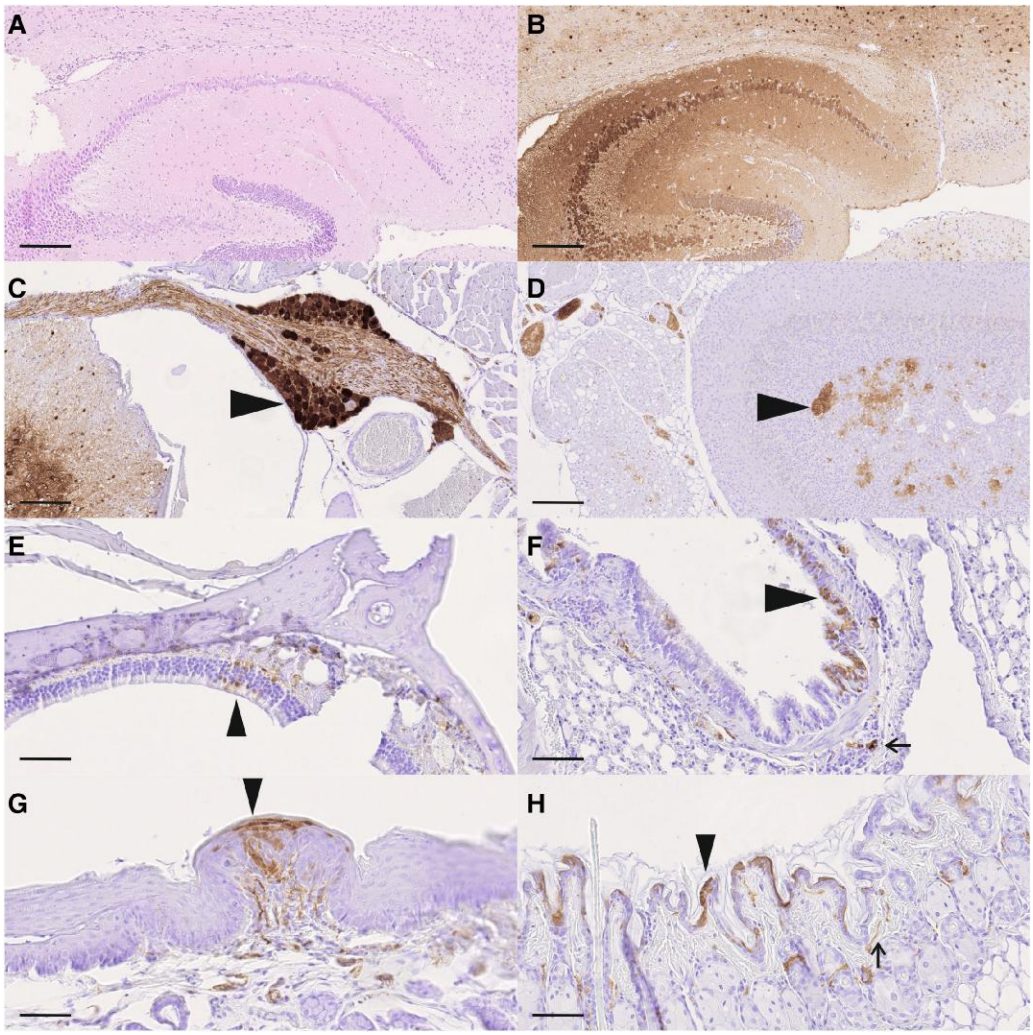


**Fig. 4.** Absence of pathological lesions demonstrated with hematoxylin and eosin stain (A), and distribution of BoDV1-N-antigen demonstrated with immunohistochemistry depicted as brown signal (B–H) in shrews experimentally infected with BoDV1. A) Intracerebrally infected shrew (H43) with no inflammatory or degenerative lesions, scale bar = 250 µm. B) Same animal as in A) with abundant BoDV1-N antigen in neurons, astrocytes, and in the neuropil, scale bar = 250 µm. C) Intracerebrally infected shrew (H49) displays BoDV1-N-antigen in spinal ganglion nuclei (arrowhead) and axons, scale bar = 100 µm. D) Adrenal gland of a subcutaneously infected shrew (H41) with BoDV1-N-antigen in medullary adrenal cells (arrowhead), scale bar = 200 µm. E) Evaluation of nasal cavity of intracerebrally infected shrew (H16) yields positive BoDV1-N-antigen in olfactory epithelial cells (arrowhead), scale bar = 100 µm. F) The lung of an intranasally infected shrew (H53) displays BoDV1-N-antigen in both cytoplasm and nuclei of bronchial epithelium (arrowhead) and submucosal nerve fibers (arrow), scale bar = 100 µm. G) Intraperitoneally infected shrew (H48) with BoDV1-N-antigen in epithelial cells of taste papillae (arrowhead), scale bar = 50 µm. H) Skin of the same animal as in F) with BoDV1-N-virus antigen in the cytoplasm of epidermal keratinocytes (arrowhead) and dermal nerve fibers (arrow), scale bar = 100 µm. BoDV1, Borna disease virus 1.

used and well characterized to date. Furthermore, neonatal rats have already been successfully used to investigate a potential immune tolerance to BoDV1 infections and showed remarkable concordance of infection results compared with the reservoir *C. leucodon* (10, 17, 18, 20, 41). To further expand knowledge on the BoDV1 infection of the reservoir, *C. russula*, the greater white-toothed shrew, was examined for its suitability as a shrew model to study the biology of bornavirus infections and their underlying pathogenesis in the reservoir. As the husbandry and breeding of *C. russula* have already been successfully established for more than 2 years, a laboratory shrew colony from comparable husbandry conditions was available in our working group.

In general, experimental BoDV1 infection of greater white-toothed shrews was successful by various routes such as intranasal, subcutaneous, intraperitoneal, and intracerebral inoculation, indicating its usefulness as animal model species. More importantly, our results support the possibility for *C. russula* to function as a natural wildlife reservoir for BoDV1, with potential of spillover to other species due to viral shedding. This observation has recently been supported by the detection of viral RNA in tissue pools from one *C. russula* individual from Germany (30). However, in comparison with the vast number of BoDV1-positive *C. leucodon* detected over time (17–19, 29, 30) and the decent number of examined *C. russula* without detection of BoDV1 infection (18, 19), this represents a rather rare but nonetheless possible event. The successful and simpler husbandry and breeding of *C. russula* and its hereby proven susceptibility to BoDV1 infection make this shrew species a suitable laboratory shrew model.

Since *C. leucodon* shrews were not available, *C. russula*, another shrew of the same genus, was used in this study. As previously mentioned, BoDV1 infections have been rarely found in *C. russula* (18, 19, 30). The initial results of this study show remarkable similarities between BoDV1 infections in *C. russula* and *C. leucodon*.

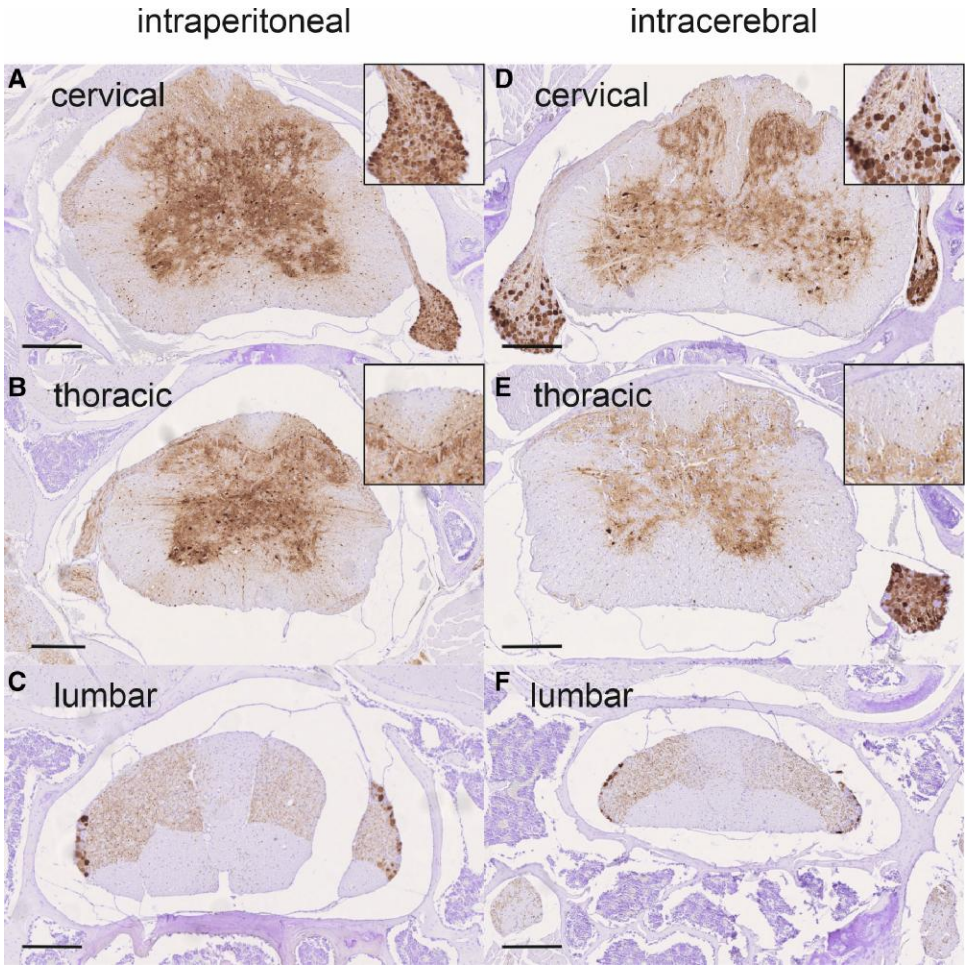


**Fig. 5.** Overview of BoDV1-N antigen distribution in the spinal cord of experimentally BoDV1-infected shrews by intraperitoneal infection (A–C) and intracerebral infection (D and E) demonstrated with immunohistochemistry depicted as brown signal. A) Cervical spinal cord of an intraperitoneally infected shrew with BoDV1-N-antigen in both gray and white matter and including motor neurons, glia cells, and surrounding neuropil as well as dorsal root ganglia (inlay), scale bar = 500 µm. B) Thoracic spinal cord of an intraperitoneally infected shrew with BoDV1-N-antigen in both gray and white matter and including motor neurons, glia cells, and surrounding neuropil as well as dorsal root ganglia. A mediodorsal triangular area within the dorsal funiculus of the spinal cord corresponding histologically to the gracile fasciculus displays hardly positive fibers (inlay), scale bar = 250 µm. C) Lumbar spinal cord of an intraperitoneally infected shrew with BoDV1-N-antigen in both gray and white matter and including motor neurons, glia cells, and surrounding neuropil, scale bar = 250 µm. D) Cervical spinal cord of an intracerebrally infected shrew with BoDV1-N-antigen in both gray and white matter and including motor neurons, glia cells, and surrounding neuropil as well as dorsal root ganglia (inlay), scale bar = 500 µm. E) Thoracic spinal cord of an intracerebrally infected shrew with BoDV1-N-antigen in both gray and white matter and including motor neurons, glia cells, and surrounding neuropil as well as dorsal root ganglia. A mediodorsal triangular area within the dorsal funiculus of the spinal cord corresponding histologically to the gracile fasciculus displays hardly positive fibers (inlay), scale bar = 250 µm. F) Lumbar spinal cord of an intracerebrally infected shrew with BoDV1-N-antigen in both gray and white matter and including motor neurons, glia cells, and surrounding neuropil, scale bar = 250 µm.

However, new insights gained from the experimental infection of *C. russula* should be cautiously extrapolated to other shrews and need to be validated whether they represent general features of BoDV1 infection in shrew species or might be rather due to species differences between *C. leucodon* and *C. russula*.

The mode of virus transmission within the shrew population as well as to dead-end hosts, such as horses and humans, is still under investigation. Former studies (18, 19) suggested the olfactory epithelium as the most likely entry site for BoDV1 infection in shrews, because it is also a plausible entry site for spillover hosts such as horses (45). Successful intranasal infection of rats in former studies (45, 46), and of greater white-toothed shrews in this study, further supports this hypothesis. However, since subcutaneous and intraperitoneal infections were also successful in *C. russula*, other or additional potential entry sites, e.g. via skin lesions and wounds, might be possible. This has also already been shown for avian bornaviruses (47). Since oral inoculation did not cause BoDV1 infection, this route of entry does not seem as likely as the other investigated inoculation routes in shrews, comparable to the transmission of avian bornaviruses (47, 48).

The presence of infectious BoDV1 in saliva and BoDV1 RNA in skin swabs and feces at 35 dpi suggests start of shedding by saliva, skin, and feces, similar to *C. leucodon* (20) and corresponding to demonstration of BoDV1 antigen in epithelial cells of salivary glands and epidermal keratinocytes. A previous study, performed on persistently BoDV1-infected bicolored white-toothed shrews by our research group, already demonstrated that *C. leucodon* shed infectious virus and RNA for a long period through saliva, skin, lacrimal fluid, urine, and feces (20). However, the shedding of BoDV1 in this study was inconsistent over the observed time course of 41 days, and therefore, other, yet unknown, factors may also influence the extent of viral shedding. In BoDV1-infected *C. russula*, viral shedding could not be detected in all animals at the end point of the experiment, which could indicate that virus

shedding starts around 35 to 41 dpi. Differences might also be due to route of infection determining the time frame for the virus to reach the peripheral organs. In summary, these data suggest that viral spread to organs capable of secretion and excretion may require about or more than 6 weeks after BoDV1 infection and may also depend on the initial entry site of the virus. Intracerebrally BoDV1-infected animals were those that already shed infectious virus via saliva on 41 dpi, while in all other groups solely viral RNA was detected in the swabs. In combination with the highest viral load in the CNS (brain and spinal cord), this argues for viral spread from the CNS to the periphery in the case of an intracerebral infection. In the case of peripheral inoculation routes, the spinal cord also harbors high viral loads, concluding that spread from periphery to the CNS to enhance viral replication and subsequent centrifugal spread to organs capable of secretion and excretions seem feasible. Notably, a mediodorsal triangular area within the dorsal funiculus of the spinal cord was relatively spared in evaluation of BoDV1-N-antigen distribution, displaying consistently less or no positive fibers (Fig. 5). No tracing studies have been conducted to characterize spinal tracts and their exact pathways and projections in *Crocidura* sp., but the area corresponds histologically to the gracile fasciculus and/or including the postsynaptic pathways of the dorsal column in mice and rats. In correlation with infection route, this might indicate that ascending sensory nerve fibers from the distal limbs are less frequently or less extensively used for BoDV1 trafficking. However, frequent positive signals in dorsal and ventral roots, extraspinal nerve fibers, ganglia ventrally to the spinal cord, as well as consistent signals in dorsal root ganglia, suggest that BoDV1 may travel along at both sensory and motor neuron axons. Nevertheless, in-depth studies of the crocidurine nervous system are needed to elucidate neural pathways and their functional aspects and to exclude differences in fiber density in the dorsal funiculus as cause for this particular observation.

Despite axonal spread to organs, neither viral RNA nor antigen was detected in the liver by qRT-PCR or immunohistochemistry, respectively. BoDV-1-infected *C. leucodon* shrews can display virus antigen in hepatic interstitial tissue, likely in nerve fibers, but not in hepatocytes (18–20), and probably only at later stages of infection. Virus antigen was not evenly distributed in the livers of these animals (20), so the absence in this study can be biased by liver sampling (a piece of the caudate lobe distant from the liver hilus). The neuroarchitecture of the liver of *C. russula* has not yet been studied intensively; therefore, a species-specific low number of nerves cannot be excluded. In rats, differences have already been shown in the neurobiology of the liver compared with other species (49). Further studies will have to show whether there are other specific hepatic metabolic processes that suppress virus distribution.

In BoDV1-infected *C. russula*, viral antigen was already present in a few clusters of epithelial cells, which might represent a prerequisite for later viral shedding. Retrograde spread from peripheral inoculation sites into the CNS, with centrifugal spread to the periphery, has already been demonstrated after peripheral inoculation of avian bornaviruses in cockatiels (50). Only few epithelial cells were BoDV1-N-antigen-positive in this study with *C. russula*, compared with former studies with *C. leucodon* (18, 19, 29), most likely indicating the beginning of viral infection of the periphery. Viral shedding increased at the end of the here presented study, concluding that a longer period of infection might be needed to establish viral spread to all organs and subsequent viral shedding via various routes in *C. russula*.

In contrast to persistently BoDV1-infected *C. leucodon* with an asymptomatic course of chronic infection (20), the experimental infection of *C. russula* led to reduced feed intake and weight loss in the acute phase. In the first week after infection, this could also be associated with anesthesia performed to conduct experimental BoDV1 inoculation, as orally, but unsuccessful inoculation similarly led to reduced feed intake. Weight loss and reduced feed intake were not associated with any morphological lesion in the CNS, or any other organ system of the animals euthanized before 41 dpi. Further studies should monitor more physiological parameters, such as body temperature or heart rate, to detect potential deviations. Furthermore, it is difficult to assess whether the observed reduced feed intake and weight loss might represent typical features of the acute phase of natural BoDV1 infections in shrews. Weight loss and starvation can enhance death and/or affect the detection of infected animals by predators. However, it is questionable whether this might explain the small numbers of naturally BoDV1-infected *C. russula* detected so far, as more factors are most likely involved. Persistence of virus in carcasses may favor transmission to predators and scavengers, but there is currently no evidence that this route is important in BoDV1 transmission as predators such as foxes only display virus-specific antibodies and no other evidence of BoDV1 infections (51). The initial body masses ranged from 10 to 15 g, and the random group assignment without factoring the body mass may have skewed the distribution of initial body mass, with larger shrews being in the oral group. Whether any other conditions of the experimental infection, such as virus dose or initial weight of the shrews, affect the course of infection and facilitate the observed clinical signs also needs to be addressed in future studies.

Interestingly, the absence of organ lesions, despite viral replication and spread in infected *C. russula*, points to a comparable virus tolerance and establishment of viral persistence as seen in *C. leucodon*. This further substantiates *C. russula* as a suitable shrew BoDV1 infection model. The reason for the absence or evasion of an antiviral immune response and virus elimination is yet unknown for the natural shrew reservoir. As Lewis rats develop a comparable pattern of virus distribution and shedding without organ lesions if they are infected as immune-incompetent newborns (41), some kind of immune tolerance seems likely in the shrew. However, since *C. russula* in this study were successfully infected as adults, different and so far, unknown mechanisms of immune tolerance might be operative in the shrew. In bats, another animal group acting as reservoir for various pathogens, many virus infections are also associated with virus tolerance and virus persistence (52, 53). Current research is revealing more and more mechanisms in bat innate immunity and disease tolerance, for example, altered tumor necrosis factor-mediated inflammation, that allows virus–host coexistence (52). Whether comparable mechanisms influence virus–host interactions in shrews needs to be addressed in future studies. Infected *C. russula* developed high serum antibody titers, comparable to the neonatally infected Lewis rats (41), indicating that the humoral antiviral response does not protect against extended viral spread and shedding, mediated by virus-specific antibodies.

The limitations of this study are that the small number of animals available allowed descriptive analyses but no valid statistical analyses. Oral inoculation did not result in successful infection, and therefore, this group served as control group but no mock infected animals were used in this study.

In summary, the successful experimental infection of *C. russula* supports their role as suitable shrew model and strengthens the status of crocidurine shrews as reservoir hosts of BoDV1 in endemic areas. The possibility of different successful infection routes suggests that several transmission pathways are possible to maintain

the virus within shrew populations. The onset of virus shedding after 5–6 weeks p.i. is indicative of the period of infection required to become an exposure risk to susceptible dead-end hosts such as humans or horses. To date, further questions remain unanswered, particularly regarding the potential immune tolerance of the shrews, the route of transmission to dead-end hosts, the long-term maintenance of BoDV1 infection in reservoir populations, and the various underlying pathogenetic mechanisms. As a prospect, this novel and successfully established shrew model can open the avenue to address these questions in future studies.

## Supplementary Material

Supplementary material is available at *PNAS Nexus* online.

## Funding

This work was supported by grants from the Federal Ministry of Education and Research project ZooBoCo (Bundesministerium für Bildung und Forschung) (Zoonotic Bornavirus Consortium), within the research network for zoonotic infectious diseases, grant number 01KI1722E/01KI2005E.

## Preprints

This manuscript was posted on a preprint: https://doi.org/10.1101/2024.07.30.605894.

## Author Contributions

D.N. was involved in conceptualization, data curation, investigation, visualization, writing—original draft, and writing—review and editing. L.R. was involved in investigation and editing. J.M. was involved in investigation, visualization, and writing—review and editing. S.H. was involved in conceptualization, resources, supervision, investigation, and writing—review and editing. M.E. was involved in conceptualization, resources, supervision, investigation, and writing—review and editing. C.H. was involved in conceptualization, resources, funding acquisition, writing—review and editing, and project administration.

## Data Availability

All data are included in the manuscript and/or Supplementary material.

## References

1 Plowright RK, *et al.* 2015. Ecological dynamics of emerging bat virus spillover. *Proc Biol Sci.* 282:20142124.
2 Daszak P, Cunningham AA, Hyatt AD. 2000. Emerging infectious diseases of wildlife—threats to biodiversity and human health. *Science.* 287:443–449.
3 Schlottau K, *et al.* 2018. Fatal encephalitic Borna disease virus 1 in solid-organ transplant recipients. *N Engl J Med.* 379:1377–1379.
4 Niller HH, *et al.* 2020. Zoonotic spillover infections with Borna disease virus 1 leading to fatal human encephalitis, 1999–2019: an epidemiological investigation. *Lancet Infect Dis.* 20:467–477.
5 Korn K, *et al.* 2018. Fatal encephalitis associated with Borna disease virus 1. *N Engl J Med.* 379:1375–1377.
6 Ebinger A, *et al.* 2024. Lethal Borna disease virus 1 (BoDV-1) infections of humans and animals—in depth molecular epidemiology and phylogeography. *Nat Commun.* 15(1):7908. doi: 10.1038/s41467-024-52192-x.
7 Liesche F, *et al.* 2019. The neuropathology of fatal encephalomyelitis in human Borna virus infection. *Acta Neuropathol.* 138:653–665.
8 Tappe D, *et al.* 2021. Investigation of fatal human Borna disease virus 1 encephalitis outside the previously known area for human cases, Brandenburg, Germany—a case report. *BMC Infect Dis.* 21:787.
9 Eisermann P, *et al.* 2021. Active case finding of current bornavirus infections in human encephalitis cases of unknown etiology, Germany, 2018–2020. *Emerg Infect Dis.* 27:1371–1379.
10 Herden C, *et al.* 2013. Bornaviridae. In: Knipe DM, Howley PM, editors. *Fields virology*. Philadelphia (PA): Lippincott Williams & Wilkins. p. 1124–1150.
11 Coras R, *et al.* 2019. Severe bornavirus-encephalitis presenting as Guillain-Barré-syndrome. *Acta Neuropathol.* 137:1017–1019.
12 Rubbenstroth D, *et al.* 2019. Human bornavirus research: back on track! *PLoS Pathog.* 15:e1007873.
13 Staeheli P. 2002. Bornaviruses. *Virus Res.* 82:55–59.
14 Malbon AJ, *et al.* 2022. New world camelids are sentinels for the presence of Borna disease virus. *Transbound Emerg Dis.* 69:451–464. https://doi.org/10.1111/tbed.14003
15 Schulze V, *et al.* 2020. Borna disease outbreak with high mortality in an alpaca herd in a previously unreported endemic area in Germany. *Transbound Emerg Dis.* 67:2093–2107.
16 Jacobsen B, *et al.* 2010. Borna disease in an adult alpaca stallion (*Lama pacos*). *J Comp Pathol.* 143:203–208.
17 Hilbe M, *et al.* 2006. Shrews as reservoir hosts of borna disease virus. *Emerg Infect Dis.* 12:675–677.
18 Bourg M, *et al.* 2013. Bicolored white-toothed shrews as reservoir for borna disease virus, Bavaria, Germany. *Emerg Infect Dis.* 19:2064–2066.
19 Dürrwald R, Kolodziejek J, Weissenböck H, Nowotny N. 2014. The bicolored white-toothed shrew *Crocidura leucodon* (HERMANN 1780) is an indigenous host of mammalian Borna disease virus. *PLoS One.* 9:e93659.
20 Nobach D, *et al.* 2015. Shedding of infectious Borna disease virus-1 in living bicolored white-toothed shrews. *PLoS One.* 10:e0137018.
21 Grabner A, Fischer A. 1991. Symptomatology and diagnosis of Borna encephalitis of horses. A case analysis of the last 13 years. *Tierarztl Prax.* 19:68–73. German.
22 Frank C, *et al.* 2022. Human Borna disease virus 1 (BoDV-1) encephalitis cases in the north and east of Germany. *Emerg Microbes Infect.* 11:6–13.
23 Bauswein M, *et al.* 2023. Human infections with Borna disease virus 1 (BoDV-1) primarily lead to severe encephalitis: further evidence from the seroepidemiological BoSOT study in an endemic region in Southern Germany. *Viruses.* 15:188. https://doi.org/10.3390/v15010188
24 Böhmer MM, *et al.* 2024. One health in action: investigation of the first detected local cluster of fatal Borna disease virus 1 (BoDV-1) encephalitis, Germany 2022. *J Clin Virol.* 171:105658.
25 Pörtner K, *et al.* 2023. Risk factors for Borna disease virus 1 encephalitis in Germany—a case-control study. *Emerg Microbes Infect.* 12:e2174778.
26 Encarnação JA, *et al.* 2013. Landscape features and reservoir occurrence affecting the risk for equine infection with Borna disease virus. *J Wildl Dis.* 49:860–868.
27 Kolodziejek J, *et al.* 2005. Genetic clustering of Borna disease virus natural animal isolates, laboratory and vaccine strains

strongly reflects their regional geographical origin. *J Gen Virol*. 86:385–398.
28 Dürrwald R, Kolodziejek J, Herzog S, Nowotny N. 2007. Meta-analysis of putative human bornavirus sequences fails to provide evidence implicating Borna disease virus in mental illness. *Rev Med Virol*. 17:181–203.
29 Puorger ME, *et al*. 2010. Distribution of Borna disease virus antigen and RNA in tissues of naturally infected bicolored white-toothed shrews, *Crocidura leucodon*, supporting their role as reservoir host species. *Vet Pathol*. 47:236–244.
30 Haring VC, *et al*. 2024. Detection of novel orthoparamyxoviruses, orthonairoviruses and an orthohepevirus in European white-toothed shrews. *Microb Genom*. 10(8):001275. doi: 10.1099/mgen.0.001275.
31 Weissenböck H, *et al*. 2017. Infections of horses and shrews with Bornaviruses in upper Austria: a novel endemic area of Borna disease. *Emerg Microbes Infect*. 6:e52.
32 Stitz L, Bilzer T, Planz O. 2002. The immunopathogenesis of Borna disease virus infection. *Front Biosci*. 7:d541–d555.
33 Tizard I, Ball J, Stoica G, *et al*. 2016. The pathogenesis of bornaviral diseases in mammals. *Anim Health Res Rev*. 17:92–109.
34 Schlohsarczyk EK, Drewes S, Koteja P, *et al*. 2023. Tropism of Puumala orthohantavirus and endoparasite coinfection in the bank vole reservoirs. *Viruses*. 15:612.
35 Genoud M. *Crocidura russula* (Hermann, 1780). In: Hausser J, editor. *Säugetiere der Schweiz: Verbreitung, Biologie, Ökologie = Mammifères de la Suisse = Mammiferi della Svizzera*. Birkäuser, Basel, 1996. p. 49–53.
36 kleinsaeuger.at. Internethandbuch über Kleinsäugerarten im mitteleuropäischen Raum: Körpermerkmale, Ökologie und Verbreitung [Internet]. Haus im Ennstal: apodemus—Institut für Wildtierbiologie. [accessed 2023 Dec 29]. https://kleinsaeuger.at/crocidura-russula/.
37 Cantoni D, Vogel P. 1989. Social organization and mating system of free-ranging, greater white-toothed shrews, *Crocidura russula*. *Anim Behav*. 38:205–214.
38 Kraft R. 2000. Ehemalige und aktuelle Verbreitung von Hausspitzmaus, *Crocidura russula* (Hermann, 1780), und Gartenspitzmaus, *Crocidura suaveolens* (Pallas, 1811) in Bayern [Former and current distribution of the greater white-toothed shrew, *Crocidura russula* (Hermann, 1780), and lesser white-toothed shrew, Crocidura suaveolens (Pallas, 1811), in Bavaria]. *Bonn Zool Beitr*. 49:115–129. German.
39 Vogel P, Jutzeler S, Rulence B, Reutter BA. 2002. Range expansion of the greater white-toothed shrew *Crocidura russula* in Switzerland results in local extinction of the bicoloured white-toothed shrew *C. leucodon*. *Acta Theriol*. 47:15–24.
40 Sikes RS. 2016. 2016 Guidelines of the American Society of Mammalogists for the use of wild mammals in research and education. *J Mammal*. 97:663–688.
41 Narayan O, *et al*. 1983. Pathogenesis of Borna disease in rats: immune-mediated viral ophthalmoencephalopathy causing blindness and behavioral abnormalities. *J Infect Dis*. 148:305–315.
42 Herzog S, Rott R. 1980. Replication of Borna disease virus in cell cultures. *Med Microbiol Immunol*. 168:153–158.
43 Petzold J, *et al*. 2019. Distribution of zoonotic variegated squirrel bornavirus 1 in naturally infected variegated and Prevost's squirrels. *Sci Rep*. 9:11402.
44 Höper D, Mettenleiter TC, Beer M. 2016. Metagenomic approaches to identifying infectious agents. *Rev Sci Tech*. 35:83–93.
45 Kupke A, Becker S, Wewetzer K, *et al*. 2019. Intranasal Borna disease virus (BoDV-1) infection: insights into initial steps and potential contagiosity. *Int J Mol Sci*. 20:1318.
46 Morales JA, *et al*. 1988. Axonal transport of Borna disease virus along olfactory pathways in spontaneously and experimentally infected rats. *Med Microbiol Immunol*. 177:51–68.
47 Heckmann J, *et al*. 2020. Wounds as the portal of entrance for parrot bornavirus 4 (PaBV-4) and retrograde axonal transport in experimentally infected cockatiels (*Nymphicus hollandicus*). *Avian Dis*. 64:247–253.
48 Heckmann J, *et al*. 2017. Investigation of different infection routes of parrot bornavirus in cockatiels. *Avian Dis*. 61:90–95.
49 Jensen KJ, Alpini G, Glaser S. 2013. Hepatic nervous system and neurobiology of the liver. *Compr Physiol*. 3:655–665.
50 Leal de Araújo J, *et al*. 2019. Distribution of viral antigen and inflammatory lesions in the central nervous system of cockatiels (*Nymphicus hollandicus*) experimentally infected with parrot bornavirus 2. *Vet Pathol*. 56:106–117.
51 Bourg M, Nobach D, Herzog S, *et al*. 2016. Screening red foxes (*Vulpes vulpes*) for possible viral causes of encephalitis. *Virol J*. 13:151.
52 Pei G, Balkema-Buschmann A, Dorhoi A. 2024. Disease tolerance as immune defense strategy in bats: one size fits all? *PLoS Pathog*. 20(9):e1012471.
53 Morales AE, *et al*. 2025. Bat genomes illuminate adaptations to viral tolerance and disease resistance. *Nature*. 638:449–458.